ISSN 1674-1056
http://cpb.iphy.ac.cn
http://iopscience.iop.org/cpb
中国物理 B
Chinese Physics
中国物理 Chinese Physics B

Wavelength dependence of intrinsic detection efficiency of NbN superconducting nanowire single-photon detector

Yong Wang(王勇), Hao Li(李浩), Li-Xing You(尤立星), Chao-Lin Lv(吕超林), He-Qing Wang(王河清), Xing-Yu Zhang(张兴雨), Wei-Jun Zhang(张伟君), Hui Zhou(周慧), Lu Zhang(张露), Xiao-Yan Yang(杨晓燕), Zhen Wang(王镇)

Citation: Chin. Phys. B . 2019, 28(7): 078502. **doi:** 10.1088/1674-1056/28/7/078502
Journal homepage: http://cpb.iphy.ac.cn; http://iopscience.iop.org/cpb

What follows is a list of articles you may be interested in

Photoinduced phase transitions in two-dimensional charge-density-wave 1T-TaS_2

Wen Wen(文雯), Chunhe Dang(党春鹤), Liming Xie(谢黎明)
Chin. Phys. B . 2019, 28(5): 058504. **doi:** 10.1088/1674-1056/28/5/058504

Responsivity and noise characteristics of AlGaN/GaN-HEMT terahertz detectors at elevated temperatures

Zhi-Feng Tian(田志锋), Peng Xu(徐鹏), Yao Yu(余耀), Jian-Dong Sun(孙建东), Wei Feng(冯伟), Qing-Feng Ding(丁青峰), Zhan-Wei Meng(孟占伟), Xiang Li(李想), Jin-Hua Cai(蔡金华), Zhong-Xin Zheng(郑中信), Xin-Xing Li(李欣幸), Lin Jin(靳琳), Hua Qin(秦华), Yun-Fei Sun(孙云飞)
Chin. Phys. B . 2019, 28(5): 058501. **doi:** 10.1088/1674-1056/28/5/058501

Ultraviolet photodetectors based on wide bandgap oxide semiconductor films

Changqi Zhou(周长祺), Qiu Ai(艾秋), Xing Chen(陈星), Xiaohong Gao(高晓红), Kewei Liu(刘可为), Dezhen Shen(申德振)
Chin. Phys. B . 2019, 28(4): 048503. **doi:** 10.1088/1674-1056/28/4/048503

Effect of temperature on photoresponse properties of solar-blind Schottky barrier diode photodetector based on single crystal Ga_2O_3

Chao Yang(杨超), Hongwei Liang(梁红伟), Zhenzhong Zhang(张振中), Xiaochuan Xia(夏晓川), Heqiu Zhang(张贺秋), Rensheng Shen(申人升), Yingmin Luo(骆英民), Guotong Du(杜国同)
Chin. Phys. B . 2019, 28(4): 048502. **doi:** 10.1088/1674-1056/28/4/048502

Realizing photomultiplication-type organic photodetectors based on C_{60}-doped bulk heterojunction structure at low bias

Wei Gong(龚伟), Tao An(安涛), Xinying Liu(刘欣颖), Gang Lu(卢刚)
Chin. Phys. B . 2019, 28(3): 038501. **doi:** 10.1088/1674-1056/28/3/038501

Wavelength dependence of intrinsic detection efficiency of NbN superconducting nanowire single-photon detector*

Yong Wang(王勇)[1,2,3], Hao Li(李浩)[1,3,†], Li-Xing You(尤立星)[1,3,‡], Chao-Lin Lv(吕超林)[1,2,3], He-Qing Wang(王河清)[1,2,3], Xing-Yu Zhang(张兴雨)[1,2,3], Wei-Jun Zhang(张伟君)[1,3], Hui Zhou(周慧)[1,3], Lu Zhang(张露)[1,2,3], Xiao-Yan Yang(杨晓燕)[1,3], and Zhen Wang(王镇)[1,3]

[1] *State Key Laboratory of Functional Materials for Informatics, Shanghai Institute of Microsystem and Information Technology (SIMIT), Chinese Academy of Sciences, Shanghai* 200050, *China*

[2] *University of Chinese Academy of Sciences, Beijing* 100049, *China*

[3] *CAS Center for Excellence in Superconducting Electronics (CENSE), Shanghai* 200050, *China*

(Received 11 March 2019; revised manuscript received 19 April 2019; published online 31 May 2019)

Superconducting nanowire single-photon detectors (SNSPDs) have attracted considerable attention owing to their excellent detection performance; however, the underlying physics of the detection process is still unclear. In this study, we investigate the wavelength dependence of the intrinsic detection efficiency (IDE) for NbN SNSPDs. We fabricate various NbN SNSPDs with linewidths ranging from 30 nm to 140 nm. Then, for each detector, the IDE curves as a function of bias current for different incident photon wavelengths of 510–1700 nm are obtained. From the IDE curves, the relations between photon energy and bias current at a certain IDE are extracted. The results exhibit clear nonlinear energy–current relations for the NbN detectors, indicating that a detection model only considering quasiparticle diffusion is unsuitable for the meander-type NbN-based SNSPDs. Our work provides additional experimental data on SNSPD detection mechanism and may serve as an interesting reference for further investigation.

Keywords: niobium nitride, superconducting nanowire single-photon detectors, detection mechanism

PACS: 85.25.Pb, 85.60.Gz **DOI:** 10.1088/1674-1056/28/7/078502

1. Introduction

Superconducting nanowire single-photon detectors (SNSPDs) have the advantages of high detection efficiency, low dark count rate, and low timing jitter, which have led to their wide used in various applications, such as quantum key distribution,[1–3] laser communication and ranging,[4–9] fluorescence spectroscopy,[10] and single photon imaging.[11] The detector performance has been considerably improved in recent years. For example, the system detection efficiency (SDE) at the wavelength of 1550 nm was raised to 93% (90%) for WSi (NbN) SNSPDs by adopting lossless optical cavities.[12,13] In the case of the timing jitter,[14–16] a timing resolution of less than 5 ps was achieved by using cryogenic amplifiers and optimizing the nanowire structures.[17] Nevertheless, the intrinsic detection mechanism of SNSPDs is not well comprehended, even though many theoretical and experimental studies have been conducted.[18–23]

When one photon is absorbed by a superconductor, it leads to the breaking up of Cooper pairs, forming a cloud of quasi-particles. Many models, such as the hot-spot model,[24] quasi-particles diffusion,[18] and vortex crossing model,[19,20,25] were applied to describe the behavior of these quasi-particles. One important technique to verify the detection model is determining the relation between the responding photon energy and bias current (I_b) at a certain responding probability. This relation is commonly referred to as the energy–current relation. A linear energy–current relation indicates that quasiparticle diffusion plays a critical role in photon response, while a nonlinear relation implies that a model considering only the quasiparticle diffusion is unsuitable and that a vortex-related detection model should be taken into consideration.[25] The linear relation was first determined for NbN-based detectors over a large range of photon energies (0.75–8.26 eV) by using quantum detector tomography (QDT).[26] Subsequently, similar results were reported for WSi-based detectors with a slight deviation from the linear behavior at low energies (0.75–0.85 eV).[27] However, other experimental results have shown nonlinear energy–current relations for WSi[25] and MoSi[28] SNSPDs. In the case of NbN SNSPDs, a nonlinear energy–current relation was also observed over a photon energy range from 0.8 eV to 2.76 eV.[25] The reported inconsistent results make the detection mechanism uncertain and thus more investigations on energy–current relations are required.

*Project supported by the National Key R&D Program of China (Grant No. 2017YFA0304000), the National Natural Science Foundation of China (Grant Nos. 61671438 and 61827823), the Science and Technology Commission of Shanghai Municipality, China (Grant No. 16JC1400402), Program of Shanghai Academic/Technology Research Leader, China (Grant No. 18XD1404600), and the Joint Research Fund in Astronomy (Grant No. U1631240) under Cooperative Agreement between the NSFC and the Chinese Academy of Sciences.

†Corresponding author. E-mail: lihao@mail.sim.ac.cn

‡Corresponding author. E-mail: lxyou@mail.sim.ac.cn

© 2019 Chinese Physical Society and IOP Publishing Ltd

In this work, the energy–current relation of NbN SNSPDs with different linewidths (30–140 nm) was studied with varying photon wavelengths (energy) from 510 nm to 1700 nm (0.73 eV to 2.43 eV). All the extracted energy–current curves show apparent nonlinear relations over the measured photon energy range. These results imply that a detection model that considers only quasiparticle diffusion is inappropriate. Our results may serve as an interesting reference for further investigation on the detection mechanism of SNSPD.

2. Device design and fabrication

We fabricated the detectors on a Si substrate with oxidized layers on both sides. A NbN thin film with a nominal thickness of 7.0 nm was deposited on the substrate at room temperature via reactive DC magnetron sputtering in a mixture of Ar (79%) and N_2 (21%) gas at a total pressure of 0.273 Pa. The sputtering current and corresponding voltage were 2.19 A and 264 V, respectively. The film thickness was controlled by the deposition time based on the calculated sputtering rate. Meander nanowire structures, covering an active circular area of diameter 5 μm, were patterned by electron beam lithography on the NbN film. The film was then reactively etched in CF_4 plasma. Finally, a bridge was etched using reactive ions to form the co-plane waveguide to enable the readout of the electrical signals. Figure 1(a) shows the schematic of the SNSPD, and the structures from top to bottom are NbN, SiO_2, and the Si substrate. As shown in Fig. 1(b) and the inset, the nanowire was patterned as meander type with width and pitch of 60 nm and 150 nm, respectively. The resulting device shows a critical temperature of 7.6 K and a square resistance 125 Ω/sq.

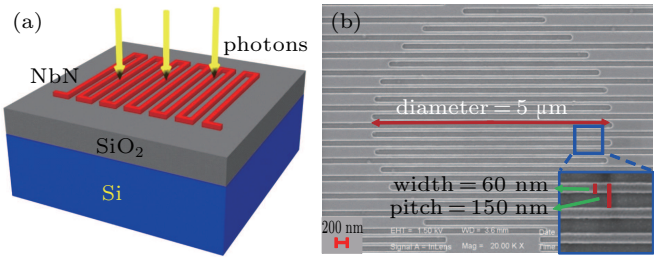


Fig. 1. (a) Schematic of a superconducting nanowire single-photon detector. (b) Scanning electron microscopy image of the surface topography of the NbN device. The active diameter of the device is 5 μm. The inset shows a magnified image of a nanowire with width and pitch of 60 nm and 150 nm, respectively.

3. Results and discussion

The device was illuminated by a HI 1060 FLEX fiber (core diameter: 6.0 ± 0.5 μm) placed in front of the device and packed in a copper sampling mount. Then, the device was installed in a Gifford–McMahon cryocooler with a working temperature of 2.100 ± 0.005 K. The bias current was applied via a quasi-constant current source,[24] and a bias-tee was utilized to separate the high-frequency detection pulses from a DC port. The device bonding with the transmission line was connected to the DC plus RF port of the bias-tee. The voltage pulse generated by the SNSPD was then amplified by a room-temperature, 50-dB gain, low noise amplifier (RF Bay Inc. LNA-650). In the optical module, the incident light was generated by a bromine–tungsten lamp. This light was passed through a grating monochromator for a series of wavelengths from 510 nm to 1700 nm. Subsequently, two attenuators were utilized to control the incident photon flux on the device.

In the experiment, we varied the incident wavelength and recorded the photon count as a function of the bias current. For each bias current, the input fiber connected with the system was blocked, and dark counts were collected for 10 s using a commercial counter. Then, the light was unblocked, and the output pulse counts were collected for another 10 s. We thus obtained the photon counts by subtracting the dark counts from the pulse counts.

The intrinsic detection efficiency (IDE) represents the pulse generation probability of the nanowire after photon absorption, which is written as IDE = PCR/ABR, where PCR is the measured photon count rate and ABR is the absorbed photon count rate. Due to the saturated SDE at high bias current, we may assume that the maximum IDE reaches unity and ABR is independent of the bias current, after which the IDE curves as a function of bias current were obtained by normalizing the SDE curves.

Figure 2 shows the dependence of IDE on the bias current for wavelengths ranging from 510 nm to 1700 nm. We observed that the nanowire starts registering photons at a bias current of approximately 4.5 μA. All of the curves show a plateau near the switching current at around $I_{SW} = 10.0$ μA. At the same current, the high photon energy results in a higher IDE, and thus, the IDE curves of short wavelengths saturated more rapidly than those of long wavelengths.

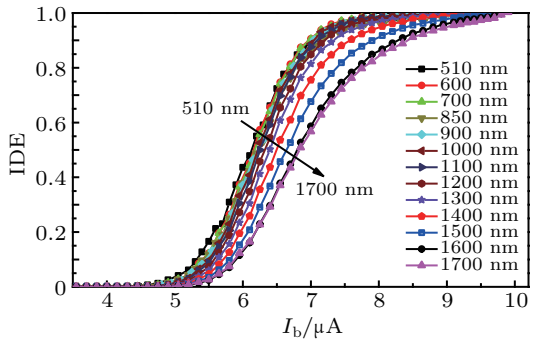


Fig. 2. Intrinsic detection efficiency as a function of bias current for wavelengths ranging from 510 nm to 1700 nm for an SNSPD linewidth of 60 nm.

We then extracted the energy–current relations from Fig. 2, as shown in Fig. 3, in which the IDE values are determined to be 1%, 30%, 50%, and 80% in comparison with previous reported works.[21,28] The curves showed nonlinear energy–current relations, which were different from the linear

relation observed in the case of QDT measurements for the NbN nanodetector.[26] Furthermore, apparent nonlinear relations were observed in the low-energy region unlike the results of a previous experimental work,[25] where only a slightly deviation from the linear relation was observed at a 50% responding probability. This result indicates that a detection mechanism model that considers only quasiparticle diffusion is incompatible with our observations.

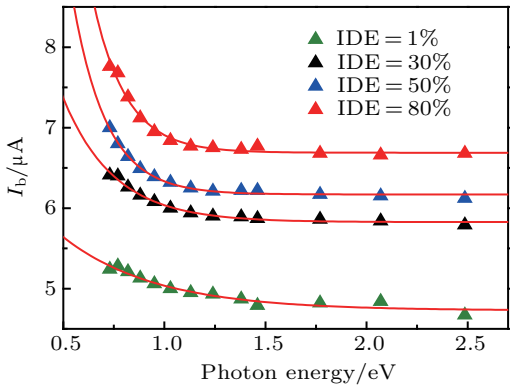


Fig. 3. Bias current as a function of incident photon energy at a response probability of 1% (green triangle), 30% (dark triangle), 50% (blue triangle), and 80% (red triangle) for an SNSPD linewidth of 60 nm. The red lines represent the fitting curves with the equation $I = I_0 + A\,\mathrm{e}^{-E/E_0}$.

To quantitatively characterize the nonlinear relations, we fitted our data using the function $I = I_0 + A\,\mathrm{e}^{-E/E_0}$, where I represents the bias current, E is the photon energy of excitation, I_0 is the reference current, and A and E_0 are constants. As shown in Fig. 3, the fitted curves coincide well with the experimental results for the IDE of 1%, 30%, 50%, and 80%, where $I_0 = 4.7$ μA, 5.8 μA, 6.2 μA, 6.7 μA, $A = 2.7$ μA, 11.3 μA, 62.3 μA, 98.1 μA, and $E_0 = 0.5$ eV, 0.3 eV, 0.2 eV, 0.2 eV, respectively. However, this formula does not fit the existing physical models.[26] Consequently, we have to admit here that this is an empirical fitting and the underlying mechanism is unclear yet.

This observation was further verified by measuring the energy–current relations of SNSPDs with linewidths of 30 nm, 80 nm, 100 nm, and 140 nm. Figure 4 shows the relation curves at 1% IDE which are all nonlinear and in good agreement with the above mentioned empirical formula. Note that for SNSPDs with linewidths of 80 nm, 100 nm, and 140 nm, PCR did not saturate at higher bias currents for long wavelengths and a sigmoid function fitting was applied to obtain the normalized IDE curve. We also noted that I_bs in the energy-current curves vary greatly for different linewidths. The smaller the nanowire width, the lower bias current at 1% response probability under the same photon energy. Indeed, various detection models of SNSPD agree with each other (at least qualitatively) on this point. For the hot-spot model, the same photon energy means the same hot-spot size. The wider nanowire needs a higher bias current to guarantee that the redistributed bias current density exceeds the critical current density and thus generate the detection event.[24] In the quasiparticles diffusion model, the current carrying capacity of the wire is proportional to the number of remaining Cooper pairs. A wider nanowire indicates a smaller quasiparticles density across the nanowire, which needs a larger bias current to guarantee that the Cooper pairs exceed the critical velocity.[18] For the vortex-crossing model, the vortex barrier is proportional to the wire width. To overcome the energy barrier, the wider nanowire needs a higher bias current to reduce the barrier.[20]

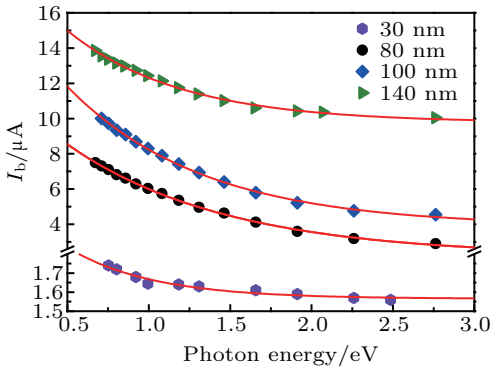


Fig. 4. Plot of bias current versus incident photon energy at 1% response probability for wire widths of 30 nm, 80 nm, 100 nm, and 140 nm. Both the experimental data and the fitting curves (red lines) follow a nonlinear energy–current relation. The fitting parameters are $I_0 = 1.6$ μA, 2.2 μA, 3.9 μA, 9.7 μA; $A = 0.7$ μA, 10.6 μA, 14.4 μA, 10.7 μA; and $E_0 = 0.5$ eV, 1.0 eV, 0.8 eV, 0.7 eV, respectively.

In previous works, linear energy–current relations were found by using QDT[26] for different types of NbN devices such as nanodetectors, nanobridges, and meanders. Similar results were also found in WSi nanobridge detectors along with a slight deviation for the range between 0.75 eV to 0.85 eV.[27] On the contrary, nonlinear relations were also observed in MoSi,[28] WSi,[25] and NbN[25] meander detectors. While the conclusion of non-linear relationship of energy–current in this paper has been drawn in previous work,[25] our work here further confirms the non-linear relationship under different nanowire widths and adds the experimental data at the width of 60 nm in the long wavelength range. In Ref. [25], the data was obtained by using extrapolation (sigmoid curve fitting) instead. Moreover, the fitting function is given in our work to quantitatively characterize the nonlinear relations. Our results indicate the nonlinear relation in NbN SNSPDs using various nanowire widths, provide additional experimental data, and may serve as an interesting reference for further investigation. Finally, it is worth noting that those discrepancies in the reported experimental results may be explained by the different photon energy range, different structures, and/or different materials and more systematically comparison is necessary before making the conclusion whether the quasiparticle diffusion model dominates the detection mechanism of SNSPD.

4. Conclusion

We studied the IDE–bias current relation of SNSPDs for different photon energies from 0.73 eV to 2.43 eV and derived the energy–current relation. A clear nonlinear relation was observed for SNSPDs with different linewidths. The results are consistent with previous reports on MoSi[28] and WSi,[25] but different from the initial results in the QDT measurements for the NbN nanodetector. However, the conclusion drawn from the linear relation may not be suitable for the detection mechanism of SNSPDs. Therefore, more systematical experimental work is necessary to determine the detection model of the SNSPDs.

Acknowledgment

The authors would like to thank L. Ma, H. Jin, and Z. Chen for the fabrication support, J. Huang and C. Zhang for the measurement instruction.

References

[1] Tang Y L, Yin H L, Chen S J, Liu Y, Zhang W J, Jiang X, Zhang L, Wang J, You L X, Guan J Y, Yang D X, Wang Z, Liang H, Zhang Z, Zhou N, Ma X, Chen T Y, Zhang Q and Pan J W 2014 *Phys. Rev. Lett.* **113** 190501

[2] Yin H L, Chen T Y, Yu Z W, Liu H, You L X, Zhou Y H, Chen S J, Mao Y, Huang M Q, Zhang W J, Chen H, Li M J, Nolan D, Zhou F, Jiang X, Wang Z, Zhang Q, Wang X B and Pan J W 2016 *Phys. Rev. Lett.* **117** 190501

[3] Liao S K, Cai W Q, Liu W Y, Zhang L, Li Y, Ren J G, Yin J, Shen Q, Cao Y, Li Z P, Li F Z, Chen X W, Sun L H, Jia J J, Wu J C, Jiang X J, Wang J F, Huang Y M, Wang Q, Zhou Y L, Deng L, Xi T, Ma L, Hu T, Zhang Q, Chen Y A, Liu N L, Wang X B, Zhu Z C, Lu C Y, Shu R, Peng C Z, Wang J Y and Pan J W 2017 *Nature* **549** 43

[4] Robinson B S, Kerman A J, Dauler E A, Barron R O, Caplan D O, Stevens M L, Carney J J, Hamilton S A, Yang J K W and Berggren K K 2006 *Opt. Lett.* **31** 444

[5] Xue L, Li Z, Zhang L, Zhai D, Li Y, Zhang S, Li M, Kang L, Chen J, Wu P and Xiong Y 2016 *Opt. Lett.* **41** 3848

[6] Zhu J, Chen Y, Zhang L, Jia X, Feng Z, Wu G, Yan X, Zhai J, Wu Y, Chen Q, Zhou X, Wang Z, Zhang C, Kang L, Chen J and Wu P 2017 *Sci. Rep.* **7** 15113

[7] Zhang S, Tao X, Feng Z J, Wu G H, Xue L, Yan X C, Zhang L B, Jia X Q, Wang Z Z, Sun J, Dong G Y, Kang L and Wu P H 2016 *Acta Phys. Sin.* **65** 188501 (in Chinese)

[8] Zhou H, He Y H, Lu C L, You L X, Li Z H, Wu G, Zhang W J, Zhang L, Liu X Y, Yang X Y and Wang Z 2018 *Chin. Phys. B* **27** 018501

[9] Yan X C, Zhu J, Zhang L B, Xing Q L, Chen Y J, Zhu H Q, Li J T, Kang L, Chen J and Wu P H 2017 *Acta Phys. Sin.* **66** 198201 (in Chinese)

[10] Yamashita T, Liu D, Miki S, Yamamoto J, Haraguchi T, Kinjo M, Hiraoka Y, Wang Z and Terai H 2014 *Opt. Express* **22** 28783

[11] Zhao Q Y , Zhu D, Calandri N, Dane A E, McCaughan A N, Bellei F, Wang H Z , Santavicca D F and Berggren K K 2017 *Nat. Photon.* **11** 247

[12] Marsili F, Verma V B, Stern J A, Harrington S, Lita A E, Gerrits T, Vayshenker I, Baek B, Shaw M D, Mirin R P and Nam S W 2013 *Nat. Photon.* **7** 210

[13] Zhang W, You L, Li H, Huang J, Lv C, Zhang L, Liu X, Wu J, Wang Z and Xie X 2017 *Sci. Chin. Phys. Mech. & Astron.* **60** 120314

[14] You L, Yang X, He Y, Zhang W, Liu D, Zhang W, Zhang L, Zhang L, Liu X, Chen S, Wang Z and Xie X 2013 *AIP Adv.* **3** 072135

[15] Calandri N, Zhao Q Y , Zhu D, Dane A and Berggren K K 2016 *Appl. Phys. Lett.* **109** 152601

[16] Cheng Y H, Gu C and Hu X L 2017 *Appl. Phys. Lett.* **111** 062604

[17] Korzh B A, Zhao Q Y , Frasca S, Allmaras J P, Autry T M, Bersin E A, Colangelo M, Crouch G M, Dane A E, Gerrits T, Marsili F, Moody G, Ramirez E, Rezac J D, Stevens M J, Wollman E E, Zhu D, Hale P D, Silverman K L, Mirin R P, Nam S W, Shaw M D and Berggren K K 2018 arXiv: 1804.06839

[18] Semenov A, Engel A, Hübers H W, Il'in K and Siegel M 2005 *Eur. Phys. J. B* **47** 495

[19] Bulaevskii L N, Graf M J, Batista C D and Kogan V G 2011 *Phys. Rev. B* **83** 144526

[20] Bulaevskii L N, Graf M J and Kogan V G 2012 *Phys. Rev. B* **85** 014505

[21] Renema J J, Frucci G, Zhou Z, Mattioli F, Gaggero A, Leoni R, de Dood M J A, Fiore A and van Exter M P 2013 *Phys. Rev. B* **87** 174526

[22] Lusche R, Semenov A, Korneeva Y, Trifonov A, Korneev A, Gol'tsman G and Hübers H W 2014 *Phys. Rev. B* **89** 104513

[23] Renema J J, Wang Q, Gaudio R, Komen I, op 't Hoog K, Sahin D, Schilling A, van Exter M P, Fiore A, Engel A and de Dood M J 2015 *Nano Lett.* **15** 4541

[24] Gol'tsman G N, Okunev O, Chulkova G, Lipatov A, Semenov A, Smirnov K, Voronov B, Dzardanov A, Williams C and Sobolewski R 2001 *Appl. Phys. Lett.* **79** 705

[25] Vodolazov D Y, Korneeva Y P, Semenov A V, Korneev A A and Goltsman G N 2015 *Phys. Rev. B* **92** 104503

[26] Renema J J, Gaudio R, Wang Q, Zhou Z, Gaggero A, Mattioli F, Leoni R, Sahin D, de Dood M J A, Fiore A and van Exter M P 2014 *Phys. Rev. Lett.* **112** 117604

[27] Gaudio R, Renema J J, Zhou Z, Verma V B, Lita A E, Shainline J, Stevens M J, Mirin R P, Nam S W, van Exter M P, de Dood M J A and Fiore A 2016 *Appl. Phys. Lett.* **109** 031101

[28] Caloz M, Korzh B, Timoney N, Weiss M, Gariglio S, Warburton R J, Schönenberger C, Renema J, Zbinden H and Bussières F 2017 *Appl. Phys. Lett.* **110** 083106